Neuron, Vol. 47, 581–592, August 18, 2005, Copyright ©2005 by Elsevier Inc. DOI 10.1016/j.neuron.2005.06.028

# Brain Mechanisms for Extracting Spatial Information from Smell

**Jess Porter,[1,5,*] Tarini Anand,[2] Brad Johnson,[2] Rehan M. Khan,[3,4,5] and Noam Sobel[1,2,3,4,*]**
[1]Program in Biophysics
[2]Program in Bioengineering
[3]Helen Wills Neuroscience Institute
[4]Department of Psychology
University of California, Berkeley
Berkeley, California 94720

## Summary

**Forty years ago, von Békésy demonstrated that the spatial source of an odorant is determined by comparing input across nostrils, but it is unknown how this comparison is effected in the brain. To address this, we delivered odorants to the left or right of the nose, and contrasted olfactory left versus right localization with olfactory identification during brain imaging. We found nostril-specific responses in primary olfactory cortex that were predictive of the accuracy of left versus right localization, thus providing a neural substrate for the behavior described by von Békésy. Additionally, left versus right localization preferentially engaged a portion of the superior temporal gyrus previously implicated in visual and auditory localization, suggesting that localization information extracted from smell was then processed in a convergent brain system for spatial representation of multisensory inputs.**

## Introduction

*"It takes little talent to see what lies under one's nose, a good deal to know in what direction to point that organ."*—W.H. Auden

Even a coarse observation of behavior reveals that mammals routinely extract spatial information from smell. Examples range from scent tracking in dogs (Thesen et al., 1993) and rats (Wallace et al., 2002) to truffle hunting in pigs (Ackerman, 1990). However, the brain structures and mechanisms that subserve the transformation of olfactory input to spatial coordinates are unknown. A common theme in mammalian sensory systems is the integration of information from bilateral receptive fields to generate spatial representations. In vision, binocular comparisons allow for depth perception (Barlow, 1967). In audition, interaural cues subserve the localization of sound sources (Knudsen and Konishi, 1979). Similarly, the possibility that mammals extract spatial information from smell by comparing input across nostrils was supported by von Békésy (1964), who, in an elegant study, found that differences in odorant concentration or in time of stimulus arrival across the two nostrils enable humans to spatially localize an odorant (1964).

To investigate the neural substrates that subserve the behavioral mechanism described by von Békésy, we set out to conduct a left versus right odorant localization study within the functional magnetic resonance (fMRI) scanner. The following considerations guided us in the selection of odorants for this task. Odor perception results from the combination of inputs from odorant transduction at a number of different nerves (Bojsen-Moller, 1975). Whereas high concentrations of most known odorants will excite the trigeminal and olfactory nerves ("trigeminal odorants"), a very small number of odorants will excite the olfactory nerve only ("pure olfactants"). Although these nerve pathways are linked at both peripheral (Bouvet et al., 1987; Schaefer et al., 2002) and central (Macrides and Chorover, 1972; Stone and Rebert, 1970; Stone et al., 1968) aspects of the olfactory system, they nevertheless induce dissociable neural responses (Hummel et al., 1992; Savic, 2002; Savic et al., 2002), and more pertinently, may contribute differently to odorant localization. Most attempts to replicate the result obtained by von Békésy have suggested that spatial localization of an odorant is possible only when the odorant is trigeminal (Kobal et al., 1989; Radil and Wysocki, 1998; Schneider and Schmidt, 1967), although some have not ruled out pure olfactory localization under some circumstances (Schneider and Schmidt, 1967). In light of this dissociation, here we chose a stimulus set that included both trigeminals (propionic acid that smells like vinegar and amyl acetate that smells like banana [Doty, 1995]) and pure olfactants (phenyl ethyl alcohol [PEA] that smells like rose and eugenol that smells like cloves [Doty, 1995]).

We used fMRI to measure neural activity in 16 human subjects during an experiment that pseudorandomly interleaved olfactory identification trials with olfactory localization (left versus right) trials (Figure 1A). Subjects wore a compartmentalized nasal mask that created a maximal olfactory spatial gradient by allowing the simultaneous presentation of odorants to one side of the nose and of clean air to the other, while still allowing for natural sniffing (Figure 2). Every 30 s, subjects heard a prompt for either "task identification" or "task localization." The prompt was followed by a tone indicating odorant onset. Subjects took one sniff and then pressed a button to indicate where the odorant was presented (right or left) for the localization task and which odorant had been presented (rose, banana, cloves, or vinegar) for the odorant identification task. Odorants and the side of presentation were pseudorandomized, counterbalanced within tasks, and equal across tasks. Nasal respiration was monitored in real time and recorded throughout the experiment.

*Correspondence: nsobel@socrates.berkeley.edu (N.S.); jessiep@calmail.berkeley.edu (J.P.)
[5]These authors contributed equally to this work.

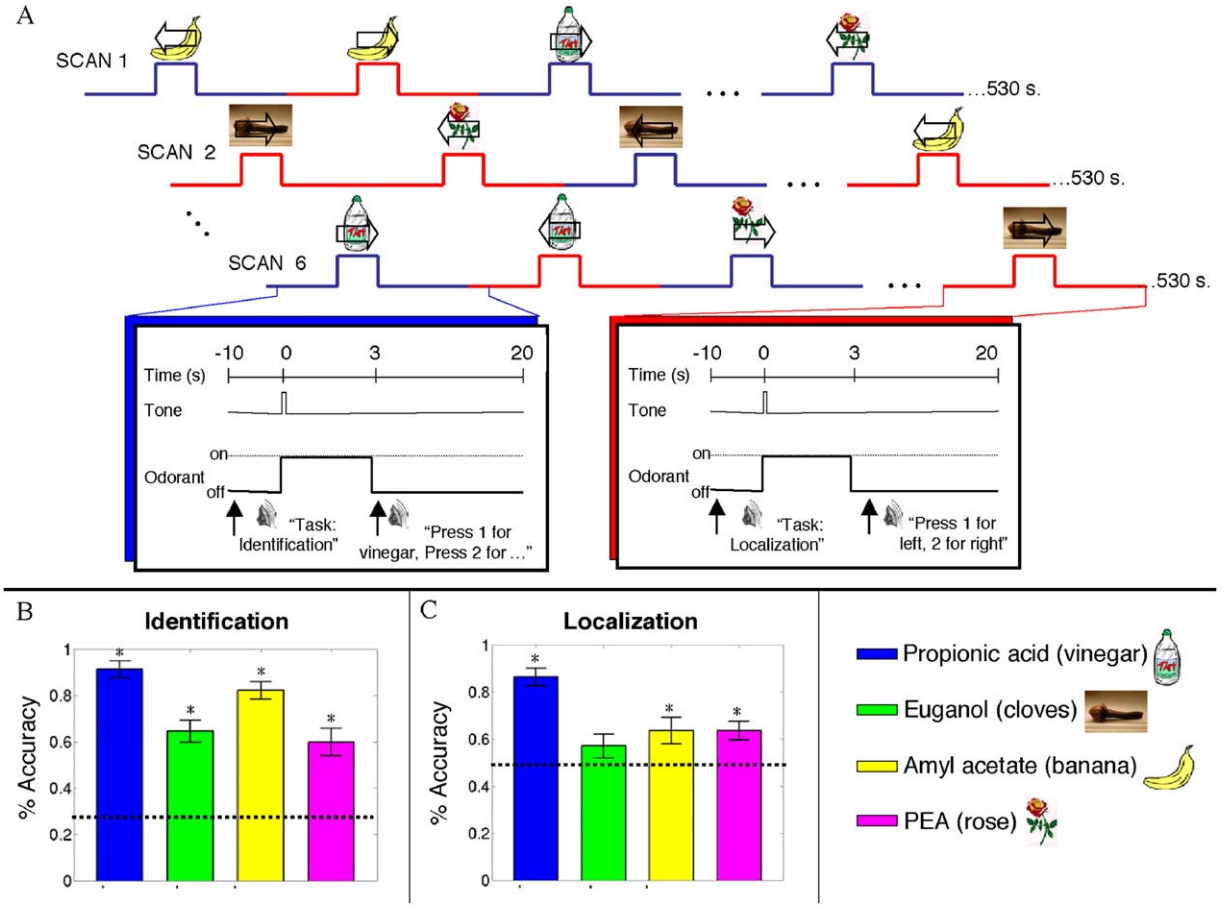


Figure 1. Experimental Design and Behavioral Accuracy

(A) Diagram of the experimental task design. Blue denotes an identification trial, and red denotes a localization trial. Note that an odorant was presented on one side of the nose on every trial. An arrow denotes the direction of presentation, and a picture denotes odorant identity.
(B) Percent accuracy in the identification task by odor. The dotted line across all odors indicates the score expected by chance, 25%.
(C) Percent accuracy in the localization task by odor. Again, the dotted line is the chance score, in this case, 50%. Error bars represent the SEM.

## Results

### Subjects Successfully Identified and Localized Odorants

Subjects were able to perform both tasks (Figures 1B and 1C). Overall identification accuracy was 74.5%, which is significantly above chance [$F(1,63) = 17$, $p < 0.0001$]. There was a difference in identification accuracy across odorants [accuracy range: 59.9%–91.3%; $F(3,63) = 10.26$, $p < 0.0001$]; however, even when considering each odorant individually, performance was significantly above chance [all $t(15) > 5$, all $p < 0.0001$]. Overall left versus right localization accuracy was 70%, which is significantly above chance [$F(1,63) = 6.56$, $p < 0.00001$]. There was again a difference in left versus right localization accuracy of the different odorants [accuracy range: 57.3%–86.4%; $F(3,63) = 56$, $p < 0.0001$]. When considering performance for each odorant separately, left versus right localization for three of the four was significantly above chance [eugenol: $t(15) = 1.4$, $p = 0.18$; all others: $t(15) > 2.3$, all $p < 0.05$]. The relatively large number of trials in this study enabled us to examine the accuracy of each subject's performance individually. Each of the 16 subjects performed accurately at levels significantly above chance in the identification task for propionic acid; 15 of 16, above chance, for eugenol (13 of them significantly so); 16 of 16, above chance, for amyl acetate (15 of them significantly so); and 14 of 16, above chance, for PEA (12 of them significantly so). At the individual level, the accuracy of 16/16 subjects was above chance for localizing propionic acid (13 of them significantly so), 7 of 16, for eugenol (five of them significantly so), 10 of 16, for amyl acetate (seven of them significantly so), and 12 of 16, for PEA (five of them significantly so).

To address the concern that successful left versus right localization may have reflected some artifactual unidentified nonolfactory cue within our apparatus, we conducted two control studies with ten additional subjects in each. To ask whether there were any auditory, tactile, or visual cues for localization, in the first control study, we removed the artificial septum that maximized

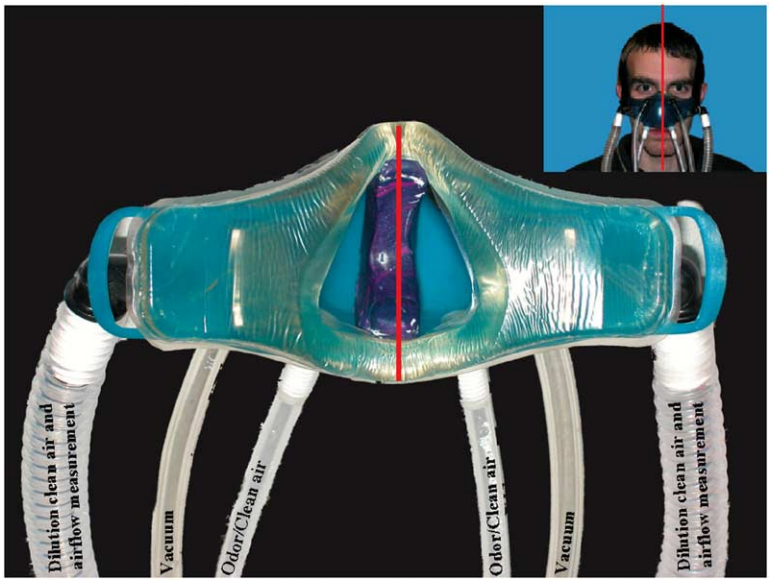


Figure 2. A Photograph of the Compartmentalized Nasal Mask

The red line drawn indicates the separation between left and right compartments that was achieved with a septum custom-fit for each subject.

the olfactory spatial gradient, yet retained all other aspects of the experiment unchanged (performed in the scanner, using the same number/order of trials, same olfactometer, flows, odorants, etc.). Using smoke for visualization of airflows revealed that this design (consisting of high airflow and no artificial septum) created significant turbulence within the mask, with no spatial gradient. Under these conditions, subjects retained an equally high ability to identify the odorants [$F(1,827) = 640$, $p < 0.0001$], but were unable to localize the odorants [$F(1,1065) = 2.36$, $p = 0.125$].

To ask whether the artificial septum added any unidentified spatial cue, in the second control study, we left the artificial septum in place but used clean air without odorants. In order to score behavior, we designated the now clean air line that was controlled by the valve previously controlling odor, as the "odor" line. To motivate subjects, we told them that they would be localizing odorants at very low intensities. Subjects were asked to indicate on which side they smelled or detected anything. Performance under these conditions was at chance, both as a group [mean score = 50%, $t(9) = 0.0003$, $p = 0.998$] and on an individual level (all $p > 0.19$). In other words, when a clean air stimulus was generated, subjects were unable to localize it. Together, these controls verified the absence of nonolfactory cues for localization in our apparatus.

To address the possibility that our "pure olfactant" conditions may have stimulated the trigeminal nerve, we repeated the identical paradigm in five subjects who had lost their sense of smell (anosmics), as verified by the University of Pennsylvania Smell Identification Test (UPSIT) (Doty et al., 1984). Considering that anosmics still have the use of their trigeminal nerve, we expected them to be able to localize trigeminal odorants, but be unable to localize pure olfactants. As predicted, the anosmic subjects were unable to localize eugenol and PEA (individually, all $p > 0.19$; as a group, $t = 0.88$, $p = 0.39$), and as a group, they were significantly different in this respect from the main normosmic study group ($x^2 = 5.96$, $p < 0.02$). Anosmics were also unable to localize amyl acetate (individually, 1 of 5, $p < 0.05$; as a group, $t = 1.1$, $p = 0.29$), but were able to localize propionic acid (individually, 4 of 5, $p < 0.05$; as a group, $t = 2.7$, $p = 0.05$). In other words, these anosmic subjects were able to localize a trigeminal odorant, but were unable to localize the pure olfactants within our apparatus. This control suggests that our eugenol and PEA conditions can, in practice, be considered pure olfactant conditions. Therefore, when normosmics were successful on these left versus right localization tasks, we can assume that their performance depended on input from the olfactory nerve.

All mammals have asymmetric airflow across nostrils so that airflow rate is often higher in one nostril (Hasegawa and Kern, 1977; Principato and Ozenberger, 1970). One may suggest that this airflow asymmetry can contribute to the extraction of spatial information from smell. To address this possibility, we compared left versus right localization accuracy with the degree of asymmetry in airflow during performance of the task. The degree of asymmetry in airflow was not related to left versus right localization accuracy for any of the four odorants (all, $p > 0.28$, see Figure S1 in the Supplemental Data available with this article online). Although this analysis does not rule out a role for airflow asymmetry in the extraction of spatial information from smell, it suggests that this asymmetry was not a factor in the current left versus right localization task. Furthermore, this result alleviated another possible concern regarding left versus right localization in this study—namely, that the magnitude of the olfactory percept can be greater in the nostril with greater air flow so that in the case of an extreme air flow-rate asymmetry, it might be possible for a subject to correctly localize an odorant to the left or right side simply by determining olfactory magnitude. This could result in a high degree of accuracy, but would not reflect a true left versus right localization behavior. This concern was partially mitigated by the outcome of postexperimental debriefings. After

the experiment, all subjects were asked to describe their strategy for localization, and none of the subjects alluded to such a "nonspatial" approach. The lack of correlation between behavioral accuracy and airflow asymmetry, however, adds an objective measure to the subjective debriefings, which together largely negated this concern.

### Activity within Nostril-Specific Receptive Fields in Primary Olfactory Cortex Predicted Left versus Right Localization Accuracy

Finding that humans can localize an odorant to the left or right within our experimental setup, we set out to ask what neural mechanisms subserve this ability. In order to achieve left versus right localization by comparing inputs across nostrils, it is vital that those inputs remain segregated and jointly impinge on a region where cells create bilateral receptive fields. Anatomical evidence (Haberly and Price, 1978; Luskin and Price, 1983), as well as single-cell recordings (Wilson, 2001), suggest such organization in the primary olfactory cortex (POC) of rats. To probe for preserved nostril-specific representation in human POC, we structurally outlined within the anatomical scan of each subject three bilateral POC subregions: frontal (PirF) and temporal (PirT) piriform cortex and an olfactory tubercle area (Tu) (Figure 3A). We chose to examine these subregions specifically because they have been implicated as being functionally heterogeneous in previous work (Gottfried et al., 2002; Zelano et al., 2005). We conducted a five-way analysis of variance (ANOVA) on the activity in each of these sROIs, considering task, subject, side of odorant presentation, trigeminality (trigeminal or pure olfactant), and accuracy as factors. Nostril-specific receptive fields were evident in the left PirT: activity in response to right-nostril stimulation was significantly higher than that for left nostril stimulation [$F(1,1026) = 7.36$, $p = 0.0068$, surviving Bonferroni-corrected threshold for six comparisons = 0.0083] (Figure 3B). Neither a main effect of trigeminality, whereby the laterality was stronger for trigeminal odorants than pure olfactants [$F(1,1026) = 5.41$, $p = 0.0202$], nor an interaction of side and trigeminality, whereby trigeminals induced relatively more activity following right nostril stimulation [$F(1,1026) = 6.55$, $p = 0.0106$], survived the Bonferroni correction. While other regions of POC and higher classical olfactory regions showed odorant-induced activation consistent with previous reports (Cerf-Ducastel and Murphy, 2001; Gottfried et al., 2002; Poellinger et al., 2001; Rolls et al., 2003; Royet et al., 2001; Savic, 2002; Small et al., 1997; Sobel et al., 2000; Zald and Pardo, 2000; Zatorre et al., 1992; Sabri et al., 2005), none of the other POC ROIs showed a difference in activation based on the side of stimulation. Thus, our behavioral results supported a role for binaral comparisons in odorant localization, and our imaging results depicted a nostril-specific response in POC, a necessary neural substrate for such binaral comparisons.

To ask whether the nostril-specific representation in the left PirT was functionally linked to odorant localization, we examined the relationship between neural activity and behavioral accuracy. There was a significant response in the left PirT for both tasks [identification: $t(10) = 8.1$, $p < 0.00001$; localization: $t(10) = 6.36$, $p < 0.0001$]. Although the left PirT had a greater overall response to task identification than to task localization [$F(1,1068) = 6.98$, $p < 0.01$], this activity was predictive of accuracy for localization trials, but not for identification trials. In other words, there was a significantly larger response to correct localization trials as compared to incorrect localization trials [$t(514) = 2.87$, $p <$

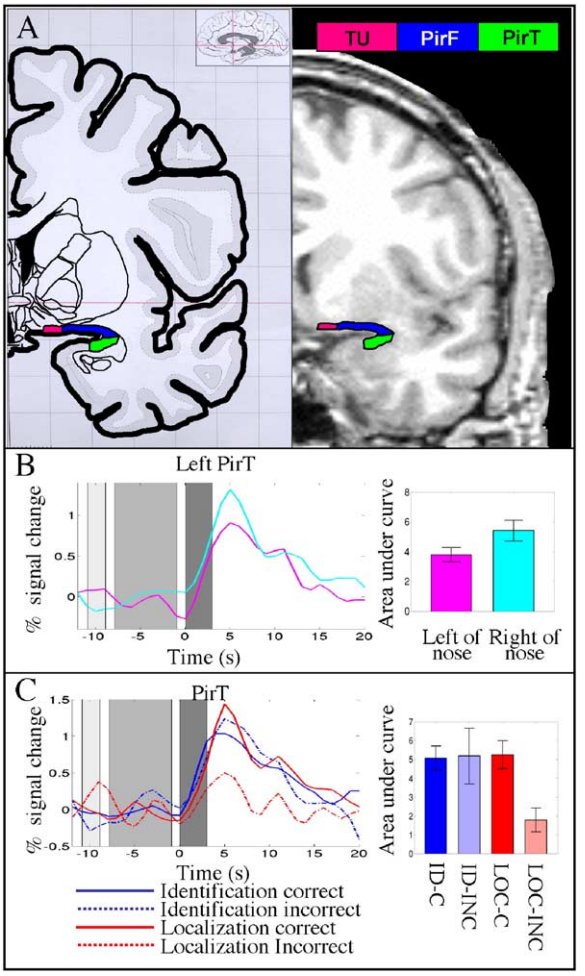


Figure 3. POC Delineation and Activation Time Course.

(A) Structural regions of interest were drawn, subdividing the piriform cortex into a tubercle region (Tu, pink), frontal region (PirF, blue), and temporal region (PirT, green). (Left panel) Atlas coronal view (Mai et al., 1997); (right panel) sample of translation to subject coronal slice.

(B and C) Group time courses: For all group (n = 16) time-course graphs (Figures 3, 5, and 6), the first light gray bar indicates the auditory instructions, "task: identification" or "task: localization"; the second medium-gray bar indicates the auditory instructions, "Please prepare to sniff at the tone, 3, 2, 1 . . . ."; and odor presentation is indicated by the dark gray bar (3 s). (B) Time course of BOLD activity in the left PirT (average ROI size in voxels = 308). Response to stimulation on the left of the nose is shown in magenta, and response to stimulation on the right of the nose is shown in cyan. At the right are bar graphs depicting the areas under the curve from t = 2–8 s. Error bars represent the SEM. (C) Time course of BOLD activity in bilateral PirT for both tasks. Note almost no activity during the incorrect localization trials.

0.005], but no difference in activity level between correct and incorrect identification trials [t(574) = −0.79, p = 0.48] (Figure 3C). That activity was predictive of behavioral accuracy strongly supports our hypothesis that this activity pattern is functionally related to odorant localization.

The nostril-specific receptive field in the left PirT was contralateral, not ipsilateral. This finding may be seen as surprising, considering that the anatomical evidence points to predominantly ipsilateral connectivity in the olfactory system (Price, 1987; Price, 1990). However, previous studies have reported bilateral convergence and processing of olfactory information (Savic and Gulyas, 2000), and this result is consistent with evidence from single-cell recordings in rat piriform cortex that ~20% of cells have contralateral receptive fields, in contrast with 15% shown to have ipsilateral receptive fields (Wilson, 2001). Thus, although the connectivity is predominantly ipsilateral, contralateral input to the POC, arising through the anterior commissure and/or other pathways, appears functionally significant.

While the results were clear in the left PirT, we did not see a mirror image of activation in the right PirT: that is, we did not see a significantly increased response to left nostril inputs. One possible reason for this negative result could be a consistently greater volume of sniffing in one nostril over the other. To address this concern, we analyzed the ongoing real-time nasal flow-rate measurements that were obtained throughout the task. Figure 4 shows average sniff traces across all subjects and conditions. As can be seen in the figure, subjects were quite good at following instructions and maintaining a consistent sniff across conditions. The only inconsistency in sniffing behavior occurred between correct and incorrect trials in each task. Subjects tended to take a longer sniff on incorrect trials, presumably because they were having difficulty and attempting to get more information. To further probe airflow sniff patterns in this study, we conducted a five-way ANOVA on both sniff volume and peak flow, with subject as a blocking variable and odorant, task, nostril, and accuracy as grouping variables. For sniff volume, there was no main effect of nostril [F(1,3230) = 0.29, p = 0.592] or task [F(1,3230) = 0.79, p = 0.37], but there was an interaction between odorant and task. Follow-up t tests revealed no difference in sniff volume for any individual odor (all p > 0.05). For peak airflow there was a very slight (2%) main effect of nostril [F(1,3230) = 4.37, p = 0.036] and no main effect of task [F(1,3230) = 0.08, p = 0.78] or interactions. This analysis negated any concerns of confounds involving sniff airflow in this study.

A second possible reason for not finding increases in activity in the right PirT during localization of odorants presented on the left may relate to the weaker overall odorant-induced response in the right compared to the left piriform regardless of task [t(2182) = 2.09, p < 0.04; Figure 5]. This translated to a lower signal-to-noise ratio in the right compared with the left piriform, and, hence, significantly reduced probability of a given voxel displaying nostril specificity. It is noteworthy that this greater odorant-induced response in the left versus the right piriform is not unique to this study (Gottfried et al., 2002; Zatorre et al., 1992) and, in consideration of the previously discussed functional significance of contralateral connectivity, may be functionally related to the slight behavioral right-nostril advantage reported in some studies of olfaction (Savic and Berglund, 2000; Zatorre and Jones-Gotman, 1990).

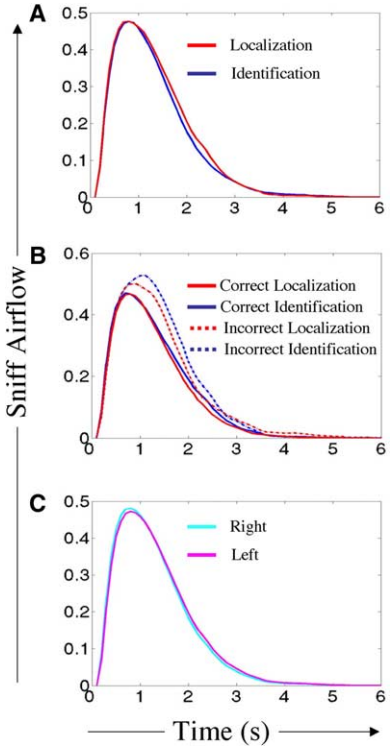


Figure 4. Sniffing

Volume versus time plots averaged across all subjects.
(A) Solid red is the average sniff trace during task: localization; solid blue is the average sniff trace during task: identification. There is no difference in sniff volume or peak flow rate between tasks.
(B) Solid red is the average sniff trace for correct localization trials, and dashed red is the average sniff trace for incorrect localization trials. Solid blue is the average sniff trace for correct identification trials, and dashed blue is the average sniff trace for incorrect identification trials. For each task, the average sniff volume on incorrect trials was greater than that on correct trials, while the peak flow was not significantly different.
(C) Magenta is the average sniff trace for the left nostril; cyan is the average sniff trace for the right nostril. The sniffs did not differ in volume, but there was a small but significant difference in peak flow.

### Activity across Specific Loci within Temporal, Parietal, and Occipital Lobes Predicted the Nature of the Task and Behavioral Accuracy

The previous analysis tested an a priori assumption regarding a mechanism for extraction of spatial information from smell by comparing input across nostrils in the POC. We now set out to investigate how this spatial information extracted from smell was further represented in the brain. In vision and audition, two distributed networks of neural substrates have been identified as preferentially subserving the encoding of spatial properties or object identity of sensory stimuli (Mishkin et al., 1983; Rauschecker and Tian, 2000; Ungerleider

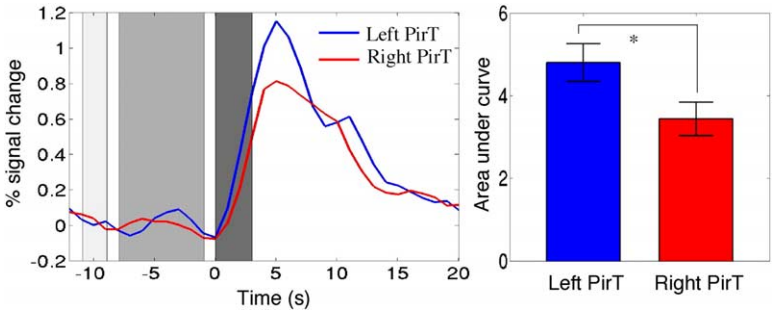


Figure 5. Time Course of BOLD Activity in the Temporal Region of Piriform Cortex

Solid red indicates the average hemodynamic response in the right PirT (330 voxels), and the average hemodynamic response in the left PirT is shown in solid blue. The response in the left PirT was greater than that in the right PirT. At the right is a bar graph showing the areas under the curves from t = 2–8 s. Error bars represent the SEM.

and Haxby, 1994). These subsystems, referred to as the "what" and "where" subsystems, follow a rough segregation into ventral and dorsal paths through the temporal and parietal lobes, respectively (Mishkin et al., 1983; Rauschecker and Tian, 2000; Ungerleider and Haxby, 1994). The current tasks of olfactory identification and localization correspond to the typical tasks used to elucidate "what" and "where" subsystems in vision and audition, so that henceforth we will switch to that terminology: "what" will refer to identification and "where," to localization. We performed a whole-brain random effects group analysis and calculated difference maps between the two conditions, "what > where" and "where > what." These analyses revealed three major regions that responded preferentially to one condition rather than the other. Specifically, the "what > where" contrast revealed activity in the occipital gyrus bilaterally (OcG), left hemisphere activation was centered at the cuneus with more extensive activation spanning several gyri in the right hemisphere (centroid = 181,151,9) (Figure 6D) and the paracentral lobule bilaterally (PCL) (Figure 6G). The "where > what" contrast revealed activity in the superior temporal gyrus (STG) bilaterally (Figure 6A) (additional responses consisting of only a few voxels were evident in ancillary regions; see Table 1). Because the group image and analysis contain an inherent loss of spatial resolution, we generated functionally restricted regions of interest (fROIs) within these anatomical loci on the anatomical images of each individual subject. The time courses of activity in these three regions are seen in Figure 6. We performed the same five-way ANOVA described in the previous section. This analysis confirmed the results of the random-effects subtraction group-image and showed that, indeed, the BOLD response in the cuneus/OcG and the PCL was greater for the "what" task than for the "where" task [cuneus/OcG: $F(1,1165) = 9.88$, $p = 0.0017$; PCL: $F(1,1254) = 5.97$, $p = 0.0147$] (Figures 6E and 6H), while the response in the STG was greater for the "where" task than for the "what" task [$F(1,1432) = 4.66$, $p = 0.0309$] (Figure 6B). It is important to note that there was no main effect of trigeminality in any of these areas, and neither was there an interaction of trigeminality with task. Therefore, we can conclude that these "what" and "where" regions were not preferentially engaged by either trigeminal or olfactory odorants, but rather were recruited in a task-specific manner independent of odor quality.

While the preceding analysis identified regions that responded differentially to the two tasks, we wanted to investigate whether this differential activity was functionally related to subjects' behavior in these tasks. To do this, we asked if the activity in any of the areas was predictive of behavioral accuracy. We found that activity in the STG was predictive of behavioral accuracy on "where" trials [$t(684) = 2.65$, $p < 0.01$] but not on "what" trials [$t(766) = 0.46$, $p = 0.646$] (Figure 6C). We found activity in the OcG to be predictive of behavioral accuracy on "what" trials [$t(574) = -2.74$, $p < 0.01$] and to approach significance on "where" trials [$t(515) = 1.85$, $p = 0.064$] (Figure 6F). Activity in the PCL was not significantly predictive of accuracy in either task (Figure 6I). These analyses of responses to correct versus incorrect trials show that neural activity within these putative "what" and "where" regions was directly related to the subject's behavior in a task-specific way. In other words, within a single subject, we could use the activity in certain brain regions to predict whether the subject would perform correctly during a certain trial, or not. Taking the idea that neural activity in these regions is an index of behavior even further, we reasoned that those subjects with greater differences between activity in these regions for correct and incorrect trials would have higher overall accuracy. To address this question, we checked the fROIs for a correlation between a subject's overall performance and the t-Statistic (or standardized population difference, an index of discriminability) between response to correct and incorrect trials. We found in the OcG a significant correlation for the identification task ($R = 0.638$, $p < 0.03$) and a trend for the localization task ($R = 0.541$, $p = 0.069$) (Figure 7). Taken together, another way of describing these results is that by observing the activity in all fROIs, one could predict what task the subject was currently performing, whether or not he/she would be likely to get the correct answer, and how accurate he/she would likely be over the entire study. This functional link between neural activity and behavior strengthens the conclusion that these regions are involved in computing odorant identity and location.

## Discussion

Sir Victor Negus, in his 1958 seminal monograph on the comparative anatomy and physiology of the nose and paranasal sinuses (Negus, 1958), noted that "the human mind is an inadequate agent with which to study olfaction, for the reason that in Man the sense of smell

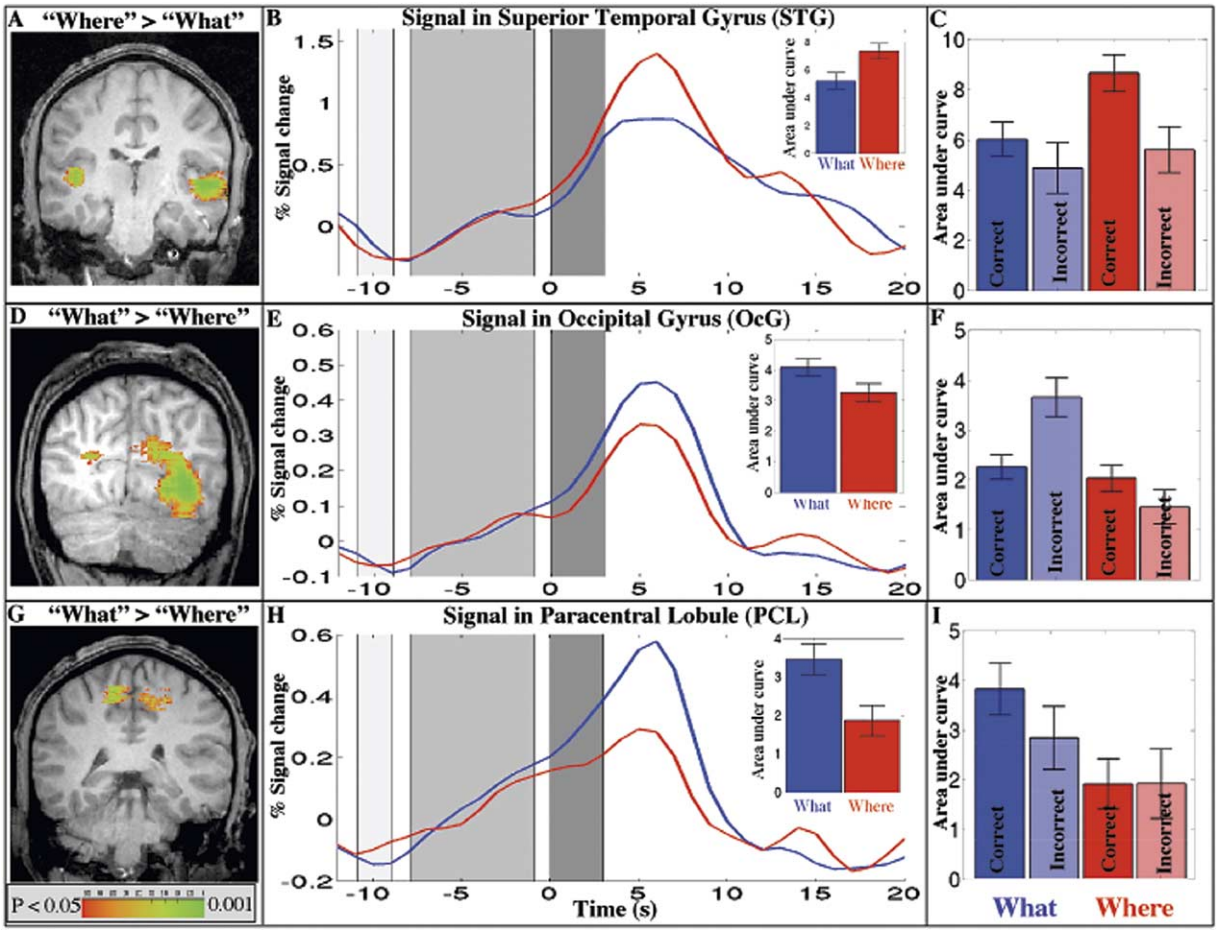


Figure 6. Task-Specific Activity Patterns

(A, D, and G) Random-effect group subtraction maps shown in coronal slices (n = 16). (A) shows the "where > what" contrast, revealing significant bilateral activity in the superior temporal gyrus. (D) and (G) show the "what > where" contrast, revealing significant bilateral activity in the occipital gyrus and the paracentral lobule.

(B, E, and H) Group time course of activity from the corresponding fROIs. "Where" trials are shown in solid red, and "what" trials, in solid blue. Bar graph inlays depict the areas under the curves of the time courses from t = 2–8 s. Error bars represent the SEM.

(C, F, and I) Areas under the curves of time-course data broken down for correct and incorrect trials.

is relatively feeble and not of great significance. It is essential, therefore, to project oneself, if possible, into the outlook of keen-scented animals in regard to their surroundings". While we disagree with Sir Negus' characterization of human olfaction (feeble and insignificant), we agree that, subjectively, olfaction plays a small part in human awareness and that this has shaped the study of olfaction by scientists. Humans do not intuitively think of olfaction as spatial. However, one look at a behaving macrosmatic mammal suggests that the olfactory stimulus is rife with spatial information. Most examples of mammalian olfactory spatial behavior, such as the aforementioned scent tracking (Thesen et al., 1993; Wallace et al., 2002) and truffle hunting (Ackerman, 1990), involve the animal moving through the olfactory space (allocentric localization). Such behavior may involve a different set of neural computations and substrates than the current example in which subjects were fixed and motionless within the olfactory space (egocentric localization) (Stoddart, 1979). The reports regarding human egocentric olfactory localization have been mixed. Whereas the successful localization of trigeminal odorants such as propionic acid is consistent with all previous results, the successful localization of relatively pure olfactants such as PEA is consistent with the results of von Békésy (1964), but not with those of others (Kobal et al., 1989; Radil and Wysocki, 1998; Schneider and Schmidt, 1967). Our explanation for this difference has to do with the behavioral profile in these studies. Whereas both we and von Békésy enabled subjects to actively sniff, other studies used tubes to passively introduce the odorant into the nostrils and either prevented sniffing altogether (Kobal et al., 1989) or enabled sniffing but with delivery via the inserted tubes (Schneider and Schmidt, 1967; Radil and Wysocki, 1998). This last-mentioned study did test one active sniffing condition and found that one of seven subjects tested was able to localize a pure olfactant (coffee). The authors noted that their failure to replicate von Békésy's results might have been due to using much weaker stim-

Table 1. ROIs Responding Preferentially to Either the Left versus Right Localization Task or the Identification Task

| ROI Name | MNI Coordinates | | | BOLD Activation | | |
|---|---|---|---|---|---|---|
| | x | y | z | "What" | "Where" | "What" – "Where" |
| Left temporal piriform | 119 | 93 | 71 | 5.7182 | 3.9206 | 1.798 |
| Right temporal piriform | 120 | 90 | 114 | 4.2188 | 2.5861 | 1.633 |
| Left frontal piriform | 113 | 89 | 69 | 3.3251 | 2.9501 | 0.375 |
| Right frontal piriform | 113 | 84 | 115 | 3.6985 | 2.4515 | 1.247 |
| Left tubercle | 113 | 92 | 82 | 3.1601 | 4.3021 | –1.142 |
| Right tubercle | 113 | 91 | 103 | 2.0242 | 3.2887 | –1.265 |
| Right cuneus/precuneus | 98 | 160 | 104 | 2.344 | 2.338 | 0.006 |
| Left cuneus | 101 | 159 | 77 | 2.157 | 1.946 | 0.212 |
| Left precuneus | 80 | 165 | 80 | 2.843 | 2.768 | 0.075 |
| Left red nucleus/superior colliculus | 112 | 116 | 88 | 2.404 | 2.301 | 0.103 |
| Right red nucleus/superior colliculus | 113 | 115 | 98 | 2.408 | 2.603 | –0.195 |
| Left superior marginal gyrus | 82 | 136 | 49 | 3.110 | 2.948 | 0.162 |
| Left inferior frontal gyrus | 87 | 62 | 66 | 6.528 | 5.774 | 0.754 |
| Right inferior frontal gyrus | 89 | 65 | 123 | 7.567 | 6.848 | 0.718 |
| Left cingulate gyrus | 75 | 88 | 85 | 4.305 | 4.166 | 0.139 |
| Right cingulate gyrus | 77 | 84 | 101 | 4.598 | 4.323 | 0.275 |
| Left precentral gyrus | 75 | 118 | 52 | 3.825 | 3.693 | 0.132 |
| Right precentral gyrus | 82 | 102 | 137 | 4.955 | 4.622 | 0.332 |
| Left short insular gyrus | 98 | 83 | 64 | 6.286 | 5.526 | 0.760 |
| Right short insular gyrus | 103 | 89 | 119 | 6.405 | 5.897 | 0.508 |
| Left frontal operculum | 88 | 94 | 44 | 5.187 | 4.746 | 0.441 |
| Right inferior temporal gyrus | 123 | 107 | 132 | 16.186 | 15.758 | 0.429 |
| Left superior temporal gyrus | 102 | 116 | 46 | 5.726 | 7.740 | –2.014 |
| Right superior temporal gyrus | 107 | 115 | 141 | 6.065 | 5.683 | 0.381 |
| Left paracentral lobule | 59 | 137 | 84 | 3.454 | 1.864 | 1.591 |
| Right paracentral lobule | 63 | 138 | 106 | 3.015 | 2.934 | 0.082 |
| Left occipital gyrus | 100 | 167 | 68 | 2.6602 | 1.847 | 0.813 |
| Right occipital gyrus | 113 | 160 | 120 | 3.920 | 2.984 | 0.935 |

BOLD activation reported is the area under the curve for the time course from time 2–8 seconds. Areas that showed a significant difference in signal across conditions are shown with gray shading ($p < 0.05$).

uli, and, hence, a spatial gradient that was not as strong. Here we maximized the spatial gradient and successfully replicated von Békésy's results. Sensory processing is an active, not a passive, process. Sniffing gives direction to the inspired air (Negus, 1958), modulates the stimulus itself as it enters the nostrils (Settles et al., 2003; Wilson and Sullivan, 1999), and plays a major role in formation of the olfactory percept (Bensafi et al., 2004; Sobel et al., 1999). Active sniffing also recruits olfactory attention (Zelano et al., 2005), and attentional allocation may then improve olfactory performance (Masago et al., 2001; Spence et al., 2001a; Spence et al., 2001b; Zelano et al., 2005). It is this enabling of near-natural behavior, namely sniffing, combined with the exaggerated spatial gradient created by the artificial septum that, in our view, enabled the behavioral profile that we observed. That said, we do not mean to assert that there is no role for the trigeminal pathway in the egocentric localization process. The behavioral results indicated that propionic acid, a strong trigeminal, was the easiest odorant for normosmic subjects to localize, and it was even localized by anosmic subjects. In contrast, eugenol, a relatively pure olfactant, was the most difficult odorant to localize. In turn, subjects were roughly equal in their ability to localize amyl acetate and PEA, despite the former having a trigeminal component and the latter being a pure olfactant.

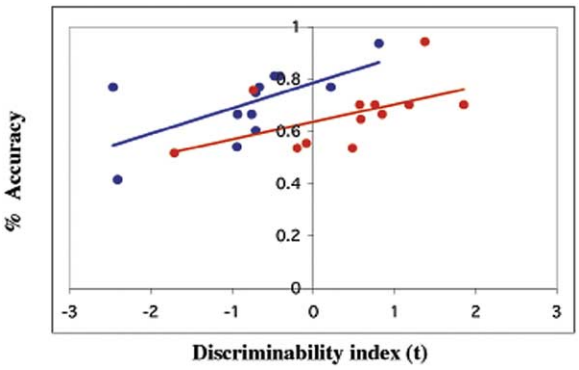


Figure 7. Neural Activity Predictive of Behavior in the left OcG

For each subject, a discriminability index (Student's t test, correct versus incorrect trials) was calculated for each task and plotted against overall accuracy (%) on that task; localization task is indicated by red and the identification task, by blue.

Olfactory localization, whether allocentric or egocentric, and whether trigeminal or pure olfactory, must be subserved by neural substrates that, to date, have not been explored. Here, we conducted such an exploration and found nostril-specific neural activity in primary olfactory cortex that was predictive of behavioral localization accuracy. As mentioned above, this activation pattern was significant only in the left PirT ROI. There are several possible reasons that we did not find a mirror activation in the right PirT: chief among them is the decreased signal-to-noise ratio in the right ROI. In addition to this primary olfactory cortex mechanism,

we found at least one significant locus of activity outside of the classical neural substrates of olfaction that was associated with olfactory localization. Specifically, activity in a particular portion of the superior temporal gyrus was greater during olfactory localization than during olfactory identification. This same region has been implicated in auditory and visual localization as well (Calvert et al., 2001), suggesting that this region may subserve crossmodal integration and transformation of sensory information to spatial coordinates. Additionally, we identified two areas preferentially activated by the identification task, a region of postcentral gyrus and a diffuse area spanning several occipital gyri. These regions are classically understood to be visual processing centers, raising the question of why they were recruited for olfactory identification. One possibility, albeit speculative, is that this activity represents the selective recruitment of olfactory visual imagery pathways during the identification task (Djordjevic et al., 2005). Measured neural activity in these regions was predictive of behavioral performance. In other words, by measuring activity in these regions, we could predict whether a subject was trying to identify or trying to localize the odorant, we could predict the likelihood of a subject's accuracy on a particular trial, and we could predict the overall accuracy of the subject on the particular task. Here, we should mention that in the case of the cuneus/OcG ROI, the activity/accuracy correlation was negative, meaning that activity inversely predicted accuracy in this region. We can only speculate on the reason for this (e.g., reduced effort); however, a correlation of either sign reflects a link between neural activity and behavior that is sufficient to imply functional significance. From our findings and from those mentioned above, we conclude that when behavioral conditions are optimized, humans can spatially localize an odorant to the left or right, this ability may be subserved by nostril-specific receptive fields within the primary olfactory cortex, as well as mechanisms of crossmodal integration in the superior temporal gyrus, that may specialize in transformation of multisensory inputs into spatial coordinates.

## Experimental Procedures

### Subjects

Sixteen normosmic subjects (eight women and eight men; age range, 22–30 years) participated in the imaging experiment, and 20 normosmic (14 women and 7 men; age range, 20–32 years) and five anosmic (four women and one man; age range, 21–34 years) subjects participated in the psychophysical control studies. All subjects gave informed consent to procedures approved by the University of California Berkeley Committee for the Protection of Human Subjects. Normosmic participants were screened for abnormal olfaction, history of neurological disease or injury, history of nasal insult (broken nose or surgery), or MR counter-indications. Anosmic subjects all scored within the "anosmic" range on the UPSIT (scores: 7, 10, 12, 12, and 16, of 40) (Doty et al., 1984).

### Odorants and Olfactometry

Odorants were delivered by a computer-controlled air-dilution olfactometer that has been previously described in detail (Johnson et al., 2003). This olfactometer switches between odorant presence and absence in less than 2 ms, with no nonolfactory cues for the alteration. The endpoint of the olfactometer is a compartmentalized nasal mask that allows for monorhinal odorant presentation. The mask design is shown in Figure 2. There are two entry ports for the odorant at the bottom of the mask, two exit ports through which the odorant is vacuumed away at an equal flow rate, and two side ports through which sniff flow-rate in the mask was measured. Measurement was by dual pneumatotachographs that provided a highly accurate constant real-time measurement of airflow in each nostril. The olfactometer, digitized auditory instruction generator, recording of respiratory data, and the MRI scanner itself, were all linked through one TTL pulse that ensures accurate time-locking of all experimental components.

### Experimental Design

This study used an event-related design (Figure 1A). There were two types of trials, task localization and task identification. Each of six scans consisted of 17 events, 1-back counter-balance for task order, with eight identification trials and nine localization trials. There was an intertrial interval of 30 s, leading to a scan length of 530 s.

Through earphones, subjects received task instructions generated by a digitally recorded voice. Each trial began with an auditory primer for "task: identification" or "task: localization." In both tasks, subjects were instructed to take one sniff at the tone. In task identification, subjects were instructed to press a button to indicate which of the four odorants had been presented. To prevent a confound of memory load, the digitized voice repeated the names of the odorants on each trial, e.g., "press one for vinegar, press two for rose, press three for banana, press four for cloves." In task localization, subjects were instructed to press a button to indicate from which side, the left or right, the odorant had been presented. On each trial, one of four odorants was presented on one side, left or right. The number of times that each odorant was presented was equal in each scan and across tasks and subjects. The only difference between trials was which task the subject was performing, identification or localization. There was no feedback to indicate performance accuracy during the scans. Subjects were instructed to try and maintain a constant sniff pattern across conditions.

### Imaging Parameters

The experiment was conducted on a 4T Varian Inova magnet. A custom-built full-head receive coil was used for signal reception. A T2* sensitive 2-shot echo planar sequence was employed with parameters of TR = 550 ms, TE = 28 ms, flip angle = 20°. Twenty 5 mm thick slices separated by 1 mm gaps were collected parallel to the AC-PC line in order to cover the entire brain using a 64 × 64 voxel matrix covering a 19.2 cm × 19.2 cm in-plane field of view, resulting in a functional in-plane resolution of 3 × 3 mm and through-plane resolution of 5 mm (for a sample slice orientation, see Figure S3). The interleaves were interpolated during image reconstruction, resulting in an effective temporal resolution of 1100 ms per frame. Fifteen frames were collected before task onset at the beginning of each scan in order to achieve dynamic equilibrium. In order to prevent head motion, a custom-formed bite bar was fit to the individual dental impression of each subject. Full brain T1-weighted flow-compensated spin-warp anatomy images (TR = 500 ms, minimum TE, isotropic 0.875 mm voxels) were acquired as a substrate on which to overlay functional data.

### Imaging Analysis

All the raw MR data will be made publicly available on our website upon publication (http://socrates.berkeley.edu/~borp/supp.htm). Data were analyzed using MrVista (http://white.stanford.edu/software/). This analysis package has been extensively developed and used to probe sensory processing with fMRI (Boynton et al., 1996; Engel et al., 1994) and has been used by us in olfaction studies (Zelano et al., 2005). First, in-plane anatomical images were aligned to the high-resolution anatomical volume of each subject's brain so that all MR images (across multiple scanning sessions) from a given subject were coregistered to an accuracy of 1 mm (Nestares and Heeger, 2000). To probe activity in the POC, prior to any functional analysis, we structurally defined three subregions, using an atlas that is particularly detailed in this respect (Mai et al., 1997). In each individual subject's volume image, we outlined bilaterally a frontal and temporal region of the piriform cortex (PirF

and PirT), as well as an olfactory tubercle region (TU). We then set out to functionally restrict each of these three subregions to only voxels that responded hemodynamically to both tasks. The average time series were converted into percent signal change by dividing each time series by its mean response and multiplying by 100. Then, the average time series for each trial within each ROI for each subject was calculated using three steps, described below.

First, for each subject we calculated an activation mask to filter out voxels for which we had no signal. We produced images of the average response across all time points at each voxel. Because voxels in gray and white matter have a significantly different mean response than do voxels in bone or air, we were able to filter voxels based on their mean response to include only voxels for which we had signal. This eliminated voxels that were in regions of high susceptibility, particularly near the ventral frontal and temporal surfaces of cortex.

Second, for each subject we produced a noise mask similar to the first that calculated the standard deviation of the response at each voxel. This mask also discriminated between regions of high susceptibility and brain tissue and further excluded voxels with high noise, such as voxels on large blood vessels.

Third, we restricted each subjects' anatomical piriform ROI to those voxels that responded to both the identification and the localization tasks. This was calculated by correlating the response at each voxel following an odorant event with a hemodynamic response function derived from the average responses of subjects in a separate study (Anderson et al., 2003). By calculating the correlation of each voxel to an expected hemodynamic response function, and the statistical significance of this correlation, we were able to produce a statistical parametric map of the responsiveness of each voxel to odorants. To restrict for responsive voxels, we excluded all voxels with a correlation to the hemodynamic response function that had a statistical significance value higher than $p = 0.05$ for both the localization and the identification tasks. To check that the task restriction was not biasing our results, we also performed restrictions for the identification task alone and the localization task alone, separately. For each subject, we computed the centroid of each resultant restricted ROI and then calculated the difference vector between the two centroids. We then conducted a one-way multivariate analysis of variance on the difference vectors and found that for all the sROIs, there was no significant difference between the two restriction types (all $p > 0.98$): that is, the regions that responded to localization and to identification in piriform cortex are not different in their location. Therefore, the results were not affected by our choice to restrict to both maps as opposed to one map at a time.

Subsequent analysis proceeded with these restricted ROIs. For each trial, a peristimulus time series (in an interval extending 20 s before sniff onset and 30 s after it) was calculated by averaging together activity across all voxels in the ROI. This time series was then smoothed with a Gaussian kernel (FWHM = 3 s) and detrended. Then, the time series was normalized by subtracting the average response from t = 20 s *before* odorant onset up to 5 s before the time of odorant onset, for the whole time series (the baseline response before sniff) so that all time series had comparable baselines. Finally, we calculated the average of all trials of a certain condition to derive an average time series for that ROI. fMRI response was defined as the area under the hemodynamic response curves in the window 2 to 8 s after odorant presentation. We then calculated the average across all trials of a given condition (in the same way described for the time courses) to get an average area under the curve for each ROI and each condition of interest. These integrals are shown as the bar graphs next to each time course. All additional analyses were then performed using the integrals of BOLD activity for each trial. In both the left versus right and 'what' versus 'where' analyses, we performed a five-way ANOVA with subjects as the blocking variable and side of odorant presentation, task, trigeminality (trigeminal or pure olfactant), and accuracy as the grouping variables. We looked for main effects as well as second-order interactions between these factors. It is noteworthy that the above-described automated noise-restriction steps eliminated the data from four subjects in the relatively MR-noisy area of the POC and OCG, two subjects in the PCL, and none in the STG. Overriding the restriction so that all subjects were retained in all analyses added significant noise, but did not eliminate any of the effects reported, so that all reported results remained significant.

For the group condition contrast analysis (Figures 6A, 6D, and 6G), we formed a composite statistical parametric map of the data for all subjects by computing activation maps within each subject's in-plane images and then aligning these images to the same brain volume. In each subject, for each voxel, we calculated four parametric maps, one for each condition, "what", "where", "what > where," and "where > what." Each voxel in each condition represented a $\beta$ parameter, obtained by regressing the response for all trials of that type against a hemodynamic response function. Each of these statistical parametric maps was then spatially smoothed (3D Gaussian kernel, FWHM = 8 mm) and transferred into the same brain volume to which the in-planes images had been aligned using a nine-parameter affine transform (Nestares and Heeger, 2000). For each voxel in the volume, we calculated a Student's t test statistic for difference from zero. This produced a random effects statistical parametric map of the significance level of each voxel (Friston et al., 1998). The statistical parametric map for responses to each condition was used with a threshold value of $p < 0.001$ to functionally define regions of interest. Although the above criteria are routinely used in fMRI without additional correction for multiple comparisons (Degonda et al., 2005; Gottfried et al., 2004; McClure et al., 2004; O'Doherty et al., 2003), to address the issue of multiple comparisons in MR data, we computed the false discovery rate (FDR) for these data (Genovese et al., 2002). The FDR using the above mentioned threshold was $q = 0.032$, an FDR below the rate recommended for fMRI (0.05) (Genovese et al., 2002). The use of FDR as a method for controlling family-wise Type I error rates is well established as a statistical method, in general (Benjamini et al., 2001) and for use in fMRI (Genovese et al., 2002; Marchini and Presanis, 2004; Welchew et al., 2005).

## Supplemental Data

Supplemental Data include three figures, Supplemental Experimental Procedures, and Supplemental References and can be found with this article online at http://www.neuron.org/cgi/content/full/cgi/47/4/581/DC1.

## Acknowledgments

Imaging studies were funded by the NIH NIDCD grant #1R01 DC006915-01. Behavioral studies were funded by ARO grant #46666-LS. The authors wish to thank Arak Elite.

Received: February 1, 2005
Revised: May 23, 2005
Accepted: June 26, 2005
Published: August 17, 2005

## References

Ackerman, D. (1990). A Natural History of the Senses (New York: Random House).

Anderson, A.K., Christoff, K., Stappen, I., Panitz, D., Ghahremani, D.G., Glover, G., Gabrieli, J.D., and Sobel, N. (2003). Dissociated neural representations of intensity and valence in human olfaction. Nat. Neurosci. *6*, 196–202.

Barlow, H.B. (1967). The neural mechanism of binocular depth discrimination. J. Physiol. *193*, 327–342.

Benjamini, Y., Drai, D., Elmer, G., Kafkafi, N., and Golani, I. (2001). Controlling the false discovery rate in behavior genetics research. Behav. Brain Res. *125*, 279–284.

Bensafi, M., Zelano, C., Johnson, B., Mainland, J., Khan, R., and Sobel, N. (2004). Olfaction: From sniff to percept. In The Cognitive Neurosciences, M. Gazzaniga, ed. (Cambridge, MA: The MIT Press), pp. 259–280.

Bojsen-Moller, F. (1975). Demonstration of terminalis, olfactory, trigeminal and perivascular nerves in the rat nasal septum. J. Comp. Neurol. *159*, 245–256.

Bouvet, J.F., Delaleu, J.C., and Holley, A. (1987). Olfactory receptor cell function is affected by trigeminal nerve activity. Neurosci. Lett. *77*, 181–186.

Boynton, G.M., Engel, S.A., Glover, G.H., and Heeger, D.J. (1996). Linear systems analysis of functional magnetic resonance imaging in human V1. J. Neurosci. *16*, 4207–4221.

Calvert, G., Hansen, P.C., Iversen, S.D., and Brammer, M.J. (2001). Detection of audio-visual integration sites in humans by application of electrophysiological criteria to the BOLD effect. Neuroimage *14*, 427–438.

Cerf-Ducastel, B., and Murphy, C. (2001). fMRI activation in response to odorants orally delivered in aqueous solutions. Chem. Senses *26*, 625–637.

Degonda, N., Mondadori, C.R., Bosshardt, S., Schmidt, C.F., Boesiger, P., Nitsch, R.M., Hock, C., and Henke, K. (2005). Implicit associative learning engages the hippocampus and interacts with explicit associative learning. Neuron *46*, 505–520.

Djordjevic, J., Zatorre, R.J., Petrides, M., Boyle, J.A., and Jones-Gotman, M. (2005). Functional neuroimaging of odor imagery. Neuroimage *24*, 791–801.

Doty, R.L. (1995). Intranasal trigeminal chemoreception. In Handbook of Olfaction and Gustation, R.L. Doty, ed. (New York: Marcel Dekker, Inc.), pp. 821–833.

Doty, R.L., Shaman, P., and Dann, M. (1984). Development of the University of Pennsylvania Smell Identification Test: a standardized microencapsulated test of olfactory function. Physiol. Behav. *32*, 489–502.

Engel, S.A., Rumelhart, D.E., Wandell, B.A., Lee, A.T., Glover, G.H., Chichilnisky, E.J., and Shadlen, M.N. (1994). fMRI of human visual cortex. [letter] Nature *369*, 525.

Friston, K.J., Fletcher, P., Josephs, O., Holmes, A., Rugg, M.D., and Turner, R. (1998). Event-related fMRI: characterizing differential responses. Neuroimage *7*, 30–40.

Genovese, C.R., Lazar, N.A., and Nichols, T. (2002). Thresholding of statistical maps in functional neuroimaging using the false discovery rate. Neuroimage *15*, 870–878.

Gottfried, J.A., Deichmann, R., Winston, J.S., and Dolan, R.J. (2002). Functional heterogeneity in human olfactory cortex: an event-related functional magnetic resonance imaging study. J. Neurosci. *22*, 10819–10828.

Gottfried, J.A., Smith, A.P., Rugg, M.D., and Dolan, R.J. (2004). Remembrance of odors past: human olfactory cortex in cross-modal recognition memory. Neuron *42*, 687–695.

Haberly, L.B., and Price, J.L. (1978). Association and commissural fiber systems of olfactory cortex of the rat. II. Systems originating in the olfactory peduncle. J. Comp. Neurol. *181*, 781–807.

Hasegawa, M., and Kern, E.B. (1977). The human nasal cycle. Mayo Clin. Proc. *52*, 28–34.

Hummel, T., Livermore, A., Hummel, C., and Kobal, G. (1992). Chemosensory event-related potentials in man: relation to olfactory and painful sensations elicited by nicotine. Electroencephalogr. Clin. Neurophysiol. *84*, 192–195.

Johnson, B.N., Mainland, J.D., and Sobel, N. (2003). Rapid olfactory processing implicates subcortical control of an olfactomotor system. J. Neurophysiol. *90*, 1084–1094.

Knudsen, E.I., and Konishi, M. (1979). Mechanisms of sound localization in the barn owl. J. Comp. Physiol. *133*, 13–21.

Kobal, G., Van Toller, S., and Hummel, T. (1989). Is there directional smelling? Experientia *45*, 130–132.

Luskin, M.B., and Price, J.L. (1983). The topographic organization of associational fibers of the olfactory system in the rat, including centrifugal fibers to the olfactory bulb. J. Comp. Neurol. *216*, 264–291.

Macrides, F., and Chorover, S.L. (1972). Olfactory bulb units: activity correlated with inhalation cycles and odor quality. Science *175*, 84–87.

Mai, J.K., Assheurer, J., and Paxinos, G. (1997). Atlas of the Human Brain (San Diego: Academic Press).

Marchini, J., and Presanis, A. (2004). Comparing methods of analyzing fMRI statistical parametric maps. Neuroimage *22*, 1203–1213.

Masago, R., Shimomura, Y., Iwanaga, K., and Katsuura, T. (2001). The effects of hedonic properties of odors and attentional modulation on the olfactory event-related potentials. J. Physiol. Anthropol. Appl. Human Sci. *20*, 7–13.

McClure, S.M., Li, J., Tomlin, D., Cypert, K.S., Montague, L.M., and Montague, P.R. (2004). Neural correlates of behavioral preference for culturally familiar drinks. Neuron *44*, 379–387.

Mishkin, M., Ungerleider, L.G., and Macko, K.A. (1983). Object vision and spatial vision: two cortical pathways. Trends Neurosci. *6*, 414–417.

Negus, S.V. (1958). The Comparative Anatomy and Physiology of the Nose and Paranasal Sinuses (London: Livingstone).

Nestares, O., and Heeger, D.J. (2000). Robust multiresolution alignment of MRI brain volumes. Magn. Reson. Med. *43*, 705–715.

O'Doherty, J.P., Dayan, P., Friston, K., Critchley, H., and Dolan, R.J. (2003). Temporal difference models and reward-related learning in the human brain. Neuron *38*, 329–337.

Poellinger, A., Thomas, R., Lio, P., Lee, A., Makris, N., Rosen, B.R., and Kwong, K.K. (2001). Activation and habituation in olfaction–an fMRI study. Neuroimage *13*, 547–560.

Price, J.L. (1987). The central olfactory and accessory olfactory systems. In Neurobiology of Taste and Smell, T.E. Finger and W.L. Silver, eds. (New York: Wiley), pp. 179–204.

Price, J.L. (1990). Olfactory system. In The Human Nervous System, G. Paxinos, ed. (San Diego: Academic Press), pp. 979–1001.

Principato, J.J., and Ozenberger, J.M. (1970). Cyclical changes in nasal resistance. Arch. Otolaryngol. *91*, 71–77.

Radil, T., and Wysocki, C.J. (1998). Spatiotemporal masking in pure olfaction. Ann. N Y Acad. Sci. *855*, 641–644.

Rauschecker, J.P., and Tian, B. (2000). Mechanisms and streams for processing of "what" and "where" in auditory cortex. Proc. Natl. Acad. Sci. USA *97*, 11800–11806.

Rolls, E.T., Kringelbach, M.L., and de Araujo, I.E. (2003). Different representations of pleasant and unpleasant odours in the human brain. Eur. J. Neurosci. *18*, 695–703.

Royet, J.P., Hudry, J., Zald, D.H., Godinot, D., Gregoire, M.C., Lavenne, F., Costes, N., and Holley, A. (2001). Functional neuroanatomy of different olfactory judgments. Neuroimage *13*, 506–519.

Sabri, M., Radnovich, A.J., Li, T.Q., and Karcken, D.A. (2005). Neural correlates of olfactory change detection. Neuroimage *25*, 969–974.

Savic, I. (2002). Imaging of brain activation by odorants in humans. Curr. Opin. Neurobiol. *12*, 455–461.

Savic, I., and Berglund, H. (2000). Right-nostril dominance in discrimination of unfamiliar, but not familiar, odours. Chem. Senses *25*, 517–523.

Savic, I., and Gulyas, B. (2000). PET shows that odors are processed both ipsilaterally and contralaterally to the stimulated nostril. Neuroreport *11*, 2861–2866.

Savic, I., Gulyas, B., and Berglund, H. (2002). Odorant differentiated pattern of cerebral activation: comparison of acetone and vanillin. Hum. Brain Mapp. *17*, 17–27.

Schaefer, M.L., Bottger, B., Silver, W.L., and Finger, T.E. (2002). Trigeminal collaterals in the nasal epithelium and olfactory bulb: a potential route for direct modulation of olfactory information by trigeminal stimuli. J. Comp. Neurol. *444*, 221–226.

Schneider, R.A., and Schmidt, C.E. (1967). Dependency of olfactory localization on non-olfactory cues. Physiol. Behav. *2*, 305–309.

Settles, G.S., Kester, D.A., and Dodson-Dreibelbis, L.J. (2003). The external aerodynamics of canine olfaction. In Sensors and Sensing in Biology and Engineering, F.G. Barth, J.A.C. Humphrey, and T.W. Secomb, eds. (New York: Springer-Verlag), pp. 323–335.

Small, D.M., Jones-Gotman, M., Zatorre, R.J., Petrides, M., and Evans, A.C. (1997). Flavor processing: more than the sum of its parts. Neuroreport *8*, 3913–3917.

Sobel, N., Khan, R.M., Saltman, A., Sullivan, E.V., and Gabrieli, J. (1999). The world smells different to each nostril. Nature *402*, 35.

Sobel, N., Prabhakaran, V., Zhao, Z., Desmond, J.E., Glover, G.H., Sullivan, E.V., and Gabrieli, J.D. (2000). Time course of odorant-induced activation in the human primary olfactory cortex. J. Neurophysiol. *83*, 537–551.

Spence, C., Kettenmann, B., Kobal, G., and McGlone, F.P. (2001a). Shared attentional resources for processing visual and chemosensory information. Q. J. Exp. Psychol. A *54*, 775–783.

Spence, C., McGlone, F.P., Kettenmann, B., and Kobal, G. (2001b). Attention to olfaction. A psychophysical investigation. Exp. Brain Res. *138*, 432–437.

Stoddart, D.M. (1979). External nares and olfactory perception. Experientia *35*, 1456–1457.

Stone, H., and Rebert, C.S. (1970). Observations on trigeminal olfactory interactions. Brain Res. *21*, 138–142.

Stone, H., Williams, B., and Carregal, E.J.A. (1968). The role of the trigeminal nerve in olfaction. Exp. Neurol. *21*, 11–19.

Thesen, A., Steen, J.B., and Doving, K.B. (1993). Behaviour of dogs during olfactory tracking. J. Exp. Biol. *180*, 247–251.

Ungerleider, L.G., and Haxby, J.V. (1994). 'What' and 'where' in the human brain. Curr. Opin. Neurobiol. *4*, 157–165.

von Békésy, G. (1964). Olfactory analogue to directional hearing. J. Appl. Physiol. *19*, 369–373.

Wallace, D.G., Gorny, B., and Whishaw, I.Q. (2002). Rats can track odors, other rats, and themselves: implications for the study of spatial behavior. Behav. Brain Res. *131*, 185–192.

Welchew, D.E., Ashwin, C., Berkouk, K., Salvador, R., Suckling, J., Baron-Cohen, S., and Bullmore, E. (2005). Functional disconnectivity of the medial temporal lobe in Asperger's syndrome. Biol. Psychiatry *57*, 991–998.

Wilson, D.A. (2001). Receptive fields in the rat piriform cortex. Chem. Senses *26*, 577–584.

Wilson, D.A., and Sullivan, R.M. (1999). Respiratory airflow pattern at the rat's snout and an hypothesis regarding its role in olfaction. Physiol. Behav. *66*, 41–44.

Zald, D.H., and Pardo, J.V. (2000). Functional neuroimaging of the olfactory system in humans. Int. J. Psychophysiol. *36*, 165–181.

Zatorre, R.J., and Jones-Gotman, M. (1990). Right-nostril advantage for discrimination of odors. Percept. Psychophys. *47*, 526–531.

Zatorre, R.J., Jones-Gotman, M., Evans, A.C., and Meyer, E. (1992). Functional localization and lateralization of human olfactory cortex. Nature *360*, 339–340.

Zelano, C., Bensafi, M., Porter, J., Mainland, J., Johnson, B., Bremner, E., Telles, C., Khan, R., and Sobel, N. (2005). Attentional modulation in human primary olfactory cortex. Nat. Neurosci. *8*, 114–120.